Structural Engineering and Mechanics, Vol. 24, No. 4 (2006) 429-446
DOI: http://dx.doi.org/10.12989/sem.2006.24.4.429

Seismic performance of RC bridge piers subjected to moderate earthquakes

Young Soo Chung† and Chang Kyu Park‡

Department of Civil Engineering, Chung-Ang University,
San 40-1, Naeri, Daedeogmyeon, Anseong Gyeonggi-Do, 456-756, Republic of Korea

Dae Hyoung Lee‡†

Department of Civil Engineering, Gyeong-Do Provincial College,
947-1, Chongbokri, Yechonup, Yechongun, Gyeongsangbukdo, 757-807, Republic of Korea

(Received September 1, 2005, Accepted June 20, 2006)

Abstract. Experimental investigation was conducted to evaluate the seismic ductility of earthquake-experienced concrete columns with an aspect ratio of 2.5. Eight circular concrete columns with a diameter of 600 mm were constructed with three test parameters: confinement ratio, lap-splice of longitudinal bars, and retrofitting with Fiber Reinforced Polymer (FRP) materials. The objective of this research is to examine the seismic performance of RC bridge piers subjected to a Quasi static test (QST), which were preliminary tested under a series of artificial earthquake motions referred to as a Pseudo dynamic test (PDT). The seismic enhancement effect of FRP wrap was also investigated on these RC bridge piers. Six specimens were loaded to induce probable damage by four series of artificial earthquakes, which were developed to be compatible with earthquakes in the Korean peninsula by the Korea Highway Corporation (KHC). Directly after the PDT, six earthquake-experienced columns were subjected to inelastic cyclic loading under a constant axial load of $0.1f_c'A_g$. Two other reference specimens without the PDT were also subjected to similar quasi-static loads. Test results showed that specimens pre-damaged by moderate artificial earthquakes generally demonstrated good residual seismic performance, which was similar to the corresponding reference specimen. Moreover, RC bridge specimens retrofitted with wrapping fiber composites in the potential plastic hinge region exhibited enhanced flexural ductility.

Keywords: RC bridge pier; seismic damage; lap splice; retrofit; transverse confinement.

1. Introduction

Korea was considered to be free of earthquake hazards since it is located relatively far away from the active fault area. However, recent earthquakes in Turkey (1999), Taiwan (1999), India (2001), Sumatra (2004), and Fukuoka (2005) have caused numerous loss of lives and extensive damage to various infrastructures. It is particularly known that Turkey (1999) and Taiwan (1999) earthquakes

† Professor
‡ Researcher, Corresponding author, E-mail: pcg2213@wm.cau.ac.kr
‡† Professor

are similar in scale, but the damage in Turkey is more severe because of the lack of seismic preparedness. Hence, to protect human lives and property from probable seismic hazard even in moderate seismic countries, enhancing seismic safety for various infrastructure systems is very important. The collapse or near collapse of bridge structures during the 1994 Northridge earthquake and the 1995 Hyogoken Nambu earthquake stimulated safety evaluations of various structures that were seismically or non-seismically designed in Korea.

RC bridges may respond elastically or in-elastically to minor or moderate earthquakes. The damage of RC columns in regions that experience inelastic action depends on the characteristics of earthquakes as well as column details. The extent of this damage affects the bridge performance during the design-level earthquake and the feasibility of restoring the column to its pre-earthquake condition. However, only relatively little research has focused on the repair of columns damaged by earthquakes. Moreover, for practical reasons lap splices were generally located in the plastic hinge region of most RC bridge columns which were constructed before the implementation of the seismic design code of the Korea highway bridge design specification (KHBDS) in 1992. Therefore, this research is aimed at investigating the effect of lap splices on the seismic performance of RC bridge piers and evaluating residual seismic performance of RC bridge piers subjected to seismic actions. The goal of this investigation was to develop an efficient strengthening method for earthquake-damaged RC piers, especially for earthquake-damaged RC bridge piers with lap-splices.

Previous research has indicated that closely spaced transverse reinforcement in the potential plastic hinge zone of bridge columns increased ultimate compression strength and strain of the concrete core. Chai *et al.* (1991) reported that the use of steel jacketing to retrofit columns was effective in restoring the flexural strength and the ductility of a damaged column, which had suffered total bond failure of the spliced reinforcement in the plastic hinge region. Saadatmanesh *et al.* (1996) experimentally studied the seismic behavior of reinforced concrete columns strengthened with fiber reinforced plastic composite straps and reported that the fiber reinforced plastic straps was very effective in confining the core concrete and preventing the longitudinal bars from buckling under cyclic loading. They also conducted an experimental investigation for the flexural behavior of four earthquake-damaged reinforced concrete columns repaired with prefabricated fiber reinforced plastic wraps, and verified the effectiveness of the proposed repair technique by showing higher flexural strength and displacement ductility of repaired columns than those of the original column. Aboutaha *et al.* (1999) have also reported the effects of confinement on the compressive strength and ductility of reinforced concrete bridge piers. They investigated the effect of lap splice lengths of the longitudinal reinforcement and repair of lap splice failures in damaged concrete columns. A total of six specimens with 18" × 36" cross-section were fabricated and tested under axial load and cyclic lateral displacement to examine the effect of two confinement steel types and different repair methods. Results from cyclic lateral load tests showed that the retrofitted columns reached their design strength and had good shear strength and ductility. Lehman *et al.* (2001) investigated experimentally the performance of earthquake-damaged reinforced concrete columns repaired by different techniques depending on the damage level and details of the original columns. Repairs for severely damaged columns used headed reinforcement, mechanical couplers, and newly cast concrete. The moderately damaged column was repaired by cover concrete patching and epoxy injection. The performance of each repair technique was determined by comparing responses of the repaired columns and original column with the design requirements.

The goal of this study is to examine the displacement ductility of RC bridge specimens with lap-spliced longitudinal reinforcement in the plastic hinge region using the Quasi-static testing (QST),

which were preliminary induced the damage of RC bridge specimens under artificial earthquake motions (Pseudo-dynamic testing, PDT) with specified Peak Ground Accelerations (PGA's). Finally, the use of FRP wrap to improve performance of these RC bridge piers with lap-spliced longitudinal reinforcement bars was examined. Eight circular test specimens with an aspect ratio of 2.5 were made with three test parameters: transverse confinement, lap splice of longitudinal bars, and retrofitting FRP materials. To provide different confinement, eight test specimens were designed in accordance with non-seismic, limited ductile, and seismic design concepts. Since lap splices of longitudinal bars in RC bridge pier are sometimes practically unavoidable, four test specimens were made with 50% of the longitudinal bars spliced. Six RC columns were damaged under PDT, and then were laterally loaded under inelastic cyclic loadings (QST) with a constant axial load ratio 0.1 of the column axial capacity. Since it is very important to estimate the residual seismic performance of RC bridge piers after a series of low and moderate earthquakes, earthquake-induced damage was simulated on these RC bridge specimens considering probable seismic ground motions in the Korean peninsula. The effect of lap splice, retrofit technique, and transverse confinement on the flexure/shear-critical RC columns was investigated. Residual seismic performance for damaged test specimens was evaluated by measuring the displacement and curvature. FRP wrapped columns showed significant improvement in seismic capacity even with lap-spliced longitudinal bars. It was concluded from the test that existing RC piers now in service, designed in accordance with the pre-1992 code as mentioned, are able to satisfy the seismic requirements of current KHBDS (Korea highway bridge design specification, 2000), when retrofitted with FRP wrapping material.

2. Test program

2.1 Test specimens

Eight circular test columns that were 0.6 m in diameter and 1.5 m in height were made as shown in Fig. 1. Four test specimens DN-SP05-R0, DN-SP05-RA, DN-SP05-RC, and DN-SP05-RG in

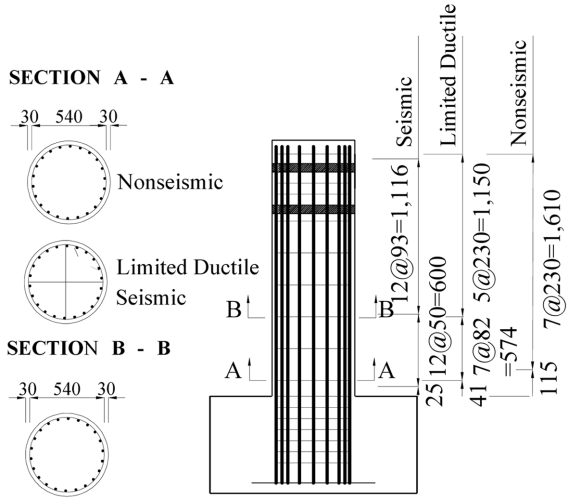

Fig. 1 Detail of test specimen

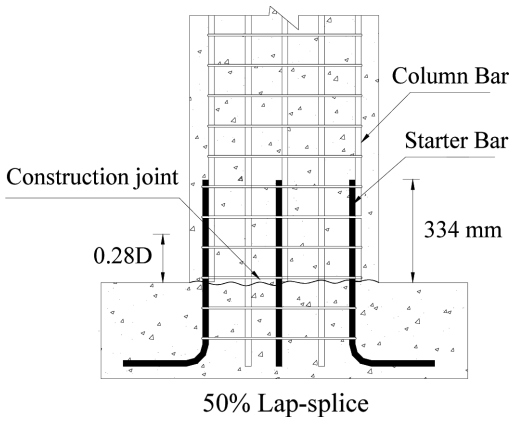

Fig. 2 Lap-spliced reinforcements

Table 1 Properties of test specimens

Design concept	Nomenclature[1]	Longitudinal steel		Confinement steel		Retrofit	Axial force (kN)
		Area ratio (%)	Lap splice	Volumetric ratio (%)	Space (mm) PHR/NPHR[2]		
Non-seismic	UN-SP00-R0	22D16 1.55%	0%	0.23	230/230	None	$0.1f_c'A_g$ = 664.4
	DN-SP00-R0						
	DN-SP50-R0		50%				
	DN-SP50-RG					SEH51	
	DN-SP50-RA					K-49	
	DN-SP50-RC					SK-N300	
Limited ductile	DL-SP00-R0		0%	0.86	82/100	None	
Seismic	US-SP00-R0			1.31	50/93	None	

1) UN=Undamaged non-seismic specimen, DN=Damaged non-seismic specimen, DL=Damaged limit ductile specimen, US=Undamaged seismic specimen, SP=Lap Splice, R=Retrofit, G=Glass (SEH-51), A=Aramid (K-49), C=Carbon (SK-N300)
2) PHR : Plastic Hinge Region, NPHR : Non Plastic Hinge Region

Table 1, were constructed using starter bars that were lapped with 50% longitudinal bars. Fig. 2 shows that longitudinal reinforcing bars of the column were extended into the footing using starter bars, which were lapped with main longitudinal reinforcing bars of the column over a length of 334 mm. This length was obtained using the equation $0.007f_y d_b$ (kgf/cm^2, cm) for the lap length of compression bars of the pre-1992 KHBDS, which was converted from the equation $0.073f_y d_b$ (MPa, mm) of AASHTO (2004). D16 deformed bar was used as the longitudinal reinforcement steels in RC test specimens and D10 deformed bar was used as the transverse confinement steels. The nominal yield strength of deformed bars is 300 MPa. Hoop reinforcement for non-seismic test specimens was overlapped in a length of 280 mm without hooks on both ends, whereas those for limited ductile and seismic test specimens were closed with a 135-degree hook on both ends. Yield strength from tensile coupon test was determined as 367 MPa for D16 deformed bar and 357 MPa for D10 deformed bar.

Achieved compressive strength, f_c', of concrete was 27 MPa. Max. aggregate size was 25 mm. As shown in Fig. 1, non-seismic test specimen DN-SP00-R0 was designed on the basis of the pre-1992 design code of KHBDS. DL-SP00-R0 and US-SP00-R0 test specimens were designed using limited ductile and full ductile concepts, respectively. UN-SP00-R0 and US-SP00-R0 specimens were not subjected to PDT as compared with other earthquake-damaged specimens. Table 1 shows details of all test specimens.

2.2 Retrofit scheme

Fiber reinforced composites have long been recognized for their high-strength, good fatigue life, light weight, ease in transportation and handling, and low maintenance costs. Fiber composites constructed of filaments such as glass, aramid, carbon, etc., are generally embedded in a resin matrix. Fibers are the primary load-carrying elements within the composite. The matrix binds the fibers together and transfers loads between them. Fibers have a strong influence on mechanical

Table 2 Mechanical properties of FRP composite straps

Fiber	Tensile strength (MPa)	Tensile modulus (MPa)	Elongation (%)	Thickness (mm)	Required thickness (mm)		Applied thickness (mm)
					Eq. (1)	Eq. (3)	
Glass (SHE-51)	571	25,714	2.0	1.3	1.12	17.68	2.60
Aramid (K-49)	2,143	112,244	2.6	0.193	0.231	4.05	0.386
Carbon (SK-N300)	3,622	239,796	1.5	0.167	0.236	1.90	0.334

properties of the composite, such as strength, elastic modulus, and deformation. The stress-strain relationship of the composite strap was linear-elastic to failure. Mechanical properties of fiber composite straps are shown in Table 2.

Three specimens DN-SP50-RA, DN-SP50-RC, and DN-SP50-RG, were strengthened using K-49, SK-N300, SEH-51, respectively, that had tensile strengths of 2,143 MPa, 3,622 MPa, and 571 MPa. Required thickness of fiber sheet can be calculated by Eq. (1) of Priestley *et al.* (1996) and Eq. (2) and (3) of Seible *et al.* (1997).

$$t_j = \frac{0.1(\varepsilon_{cu} - 0.004)Df'_{cc}}{f_{uj}\varepsilon_{uj}} \tag{1}$$

$$t_j = \frac{0.09(\varepsilon_{cu} - 0.004)Df'_{cc}}{\phi_f f_{uj}\varepsilon_{uj}} \tag{2}$$

$$t_j = 500\frac{D(f_l - f_h)}{E_j} \tag{3}$$

where, t_j is the thickness of fiber sheet, ε_{cu} and ε_{uj} are the ultimate strain of confined concrete and fiber sheet, respectively. D is the diameter of test specimen. f'_{cc} and f_{uj} are the maximum stress of confined concrete and the ultimate stress of fiber sheets, respectively. ϕ_f is the flexural capacity reduction factor. f_ℓ is the lateral clamping pressure, and f_h is the horizontal stress level provided by existing hoop reinforcement in a circular column at a strain of $1{,}000\mu\varepsilon$.

It is noted that Eq. (1) and Eq. (2) are identical when the flexural capacity reduction factor ϕ_f is typically taken as 0.9, and Eq. (3) is suggested for the retrofit of RC piers with 100% of the longitudinal bars lap-spliced. However, Chung *et al.* (2004) previously reported that the column with 50% longitudinal bars spliced was retrofitted based on the Eq. (1) and exhibited similar performance of the seismically designed columns. Thus, Eq. (1) was used for the retrofit of specimens with 50% of the longitudinal bars lap-spliced in this research. Required thickness of glass, carbon, and aramid fiber were computed as shown in Table 2. Considering unit thickness of manufactured fiber sheets, two layers of fiber sheets were applied for retrofit for three non-seismic specimens with lap-spliced longitudinal bars. Three non-seismic test specimens with 50% longitudinal bars lap-spliced were wrapped around 750 mm above the top of the footing. After the strap was wrapped around the column, epoxy was applied to the surface of the strap and multiple layers of the strap were adhered together to form a single composite wrap of the desired thickness.

2.3 Test setup and instrumentation

Since all test columns were cantilevers, the test setup was designed for testing column-footing assemblages subjected to a combination of axial and lateral loadings. Two independent loading

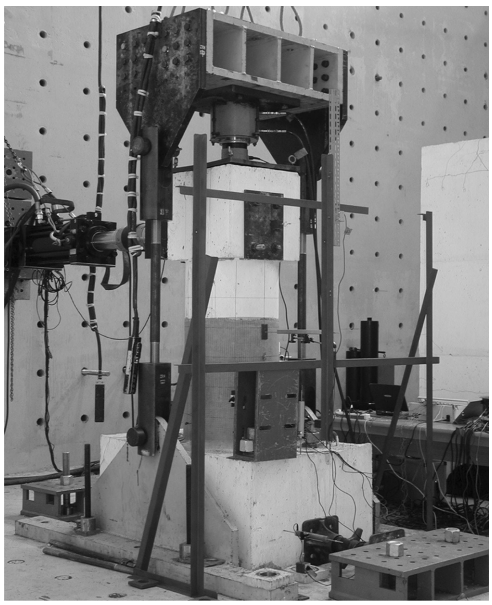

Photo 1. Test setup

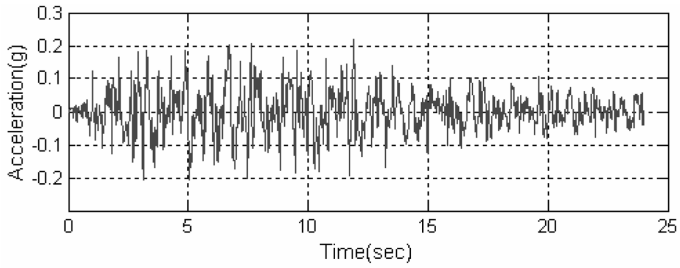

(a) Ground motions in time domain

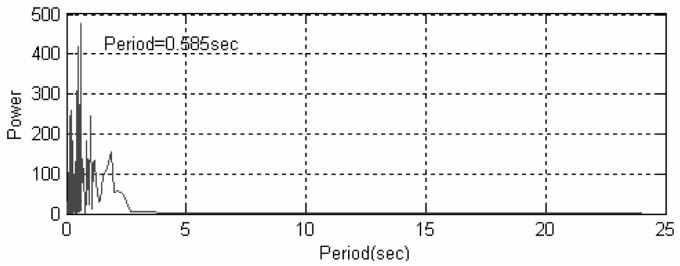

(b) Power spectrum of ground motions

Fig. 3 Input earthquake motions for PDT

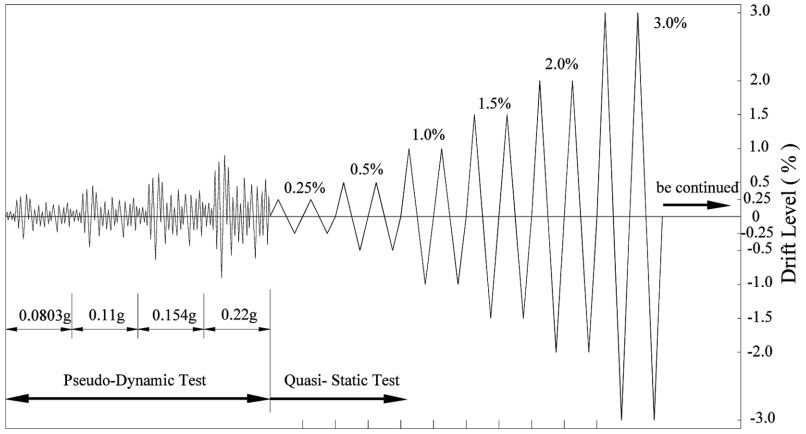

Fig. 4 Loading procedures for PDT and QST

systems are shown in Photo 1. The constant axial load of 664.4 kN (calculated from the equation $P = 0.1 f_c' A_g$) was applied to the top surface of the column, by pre-stressing a pair of high-strength steel rods against the reinforced deep floor via the loading frame. Repeated lateral forces were simultaneously applied to the column by a 1,000 kN hydraulic actuator mounted on the reaction wall. Each test column was instrumented to monitor applied displacements and their corresponding loads, strains, and deformations. Various measurements were obtained using (a) calibrated load cell and displacement transducer of the actuator, (b) clip gages and inclinometers mounted on the plastic hinge region of the column to measure the curvature, (c) displacement transducers installed on the reference frame, and (d) electrical-resistance strain gages bonded to reinforcing bars.

2.4 Loading pattern

The experimental program consisted of two load procedures: the PDT for the induction of probable damage under expected seismic ground motions in the Korean peninsula as shown in Fig. 3, and the subsequent QST for the evaluation and enhancement of residual seismic performance of earthquake-damaged RC bridge piers. Six test columns were pseudo-dynamically loaded and damaged by four series of artificial earthquake motions with different PGA values, which were developed using the seismic design provision of KHBDS. Peak ground acceleration for four input ground motions were 0.0803 g, 0.11 g, 0.154 g, and 0.22 g which respectively corresponded to 200, 500, 1000, and 2000 year return periods. The PDT is similar to a series of standard step-by-step linear analyses. Newmark's explicit β method is used for the algorithm of this PDT. As shown in Fig. 3(b), the dominant period of input ground motion is determined as 0.585 sec.

Directly after the PDT, the QST was carried out in a displacement-controlled way. As shown in Fig. 4, the displacement-controlled test was conducted on the basis of applied drift levels, starting at ±0.25%, and increased to ±0.5%, ±1.0%, ±1.5%, ±2.0%, ±2.5%, ±3.0%, ±4.0%, … to failure. The drift level was computed as the ratio of input displacement to column height.

3. Test results and discussions

3.1 Load-vs-displacement response

3.1.1 Pseudo dynamic test

All test specimens showed that cracks were concentrated within the plastic hinge region of the columns. The first earthquake with a PGA of 0.0803 g produced initial flexural cracks that were distributed over a length of 370 mm ~ 400 mm above the footing. Even after the completion of the pseudo-dynamic test, all test specimens did not yield, since maximum displacements of Table 3 were less than corresponding yield displacements of Table 4. However, many hair cracks were observed in the plastic hinge region after PDT, that seemed to be near the yield state. Concrete cracks could not be observed in retrofitted specimens due to the fiber sheets. As shown in Fig. 5, the two specimens, DN-SP00-R0 and DL-SP00-R0, without a lap splice behaved almost linearly up to the earthquake motion with a PGA of 0.22 g, regardless of different transverse confinement. All three retrofitted specimens DN-SP50-RG, DN-SP50-RA, and DN-SP50-RC exhibited a response similar to elastic behavior. As shown in Fig. 5, all test specimens including un-retrofitted and lap-spliced specimen DN-SP50-R0 elastically behaved under the PDT.

3.1.2 Quasi-static test

Most specimens failed due to the buckling and fracture of longitudinal reinforcing bars except for the two specimens UN-SP00-R0 and DN-SP00-R0, which showed a shear failure mode without the fracture of longitudinal bars.

Specimen UN-SP00-R0 showed initial flexural cracking at 0.25% drift and the cold joint cracked between column and footing at 0.5% drift. In addition, longitudinal cracks were initiated at 2.0% drift and cover concrete spalled off at 2.5% drift. At 4% drift, significant diagonal cracks occurred and this caused rapid reduction of the load-carrying capacity.

Specimen DN-SP00-R0 showed longitudinal cracks at 1.5% drift, which occurred earlier than the specimen UN-SP00-R0 at 2% drift. At 5% drift, significant diagonal cracks were observed which lead to column failure without the fracture of longitudinal bars. The failure was typical of a flexural-shear failure mode. Specimen DN-SP50-R0 with a lap splice showed that cover concrete spalled off at 3% drift and longitudinal bar fractured at 5.0% drift. At 5% drift, lap-splice failed. Limited ductile specimen DL-SP00-R0 showed more ductile behavior. Initial fracture of longitudinal bar occurred at 7.0% drift.

Table 3 Maximum force and displacement under PDT

Specimens	0.0803 g		0.11 g		0.154 g		0.22 g	
	Force (KN)	Displacement (mm)	Force (KN)	Displacement (mm)	Force (KN)	Displacement (mm)	Force (KN)	Displacement (mm)
DN-SP00-R0	148	3.19	171	4.15	193	5.33	228	7.33
DN-SP50-R0	133	3.19	155	3.98	181	5.35	218	7.65
DN-SP50-RG	149	2.52	210	4.20	247	5.84	295	8.98
DN-SP50-RA	172	2.39	224	3.76	264	5.39	318	8.33
DN-SP50-RC	153	2.92	197	4.42	242	6.32	265	8.10
DL-SP00-R0	154	3.28	172	4.25	197	5.71	226	7.64

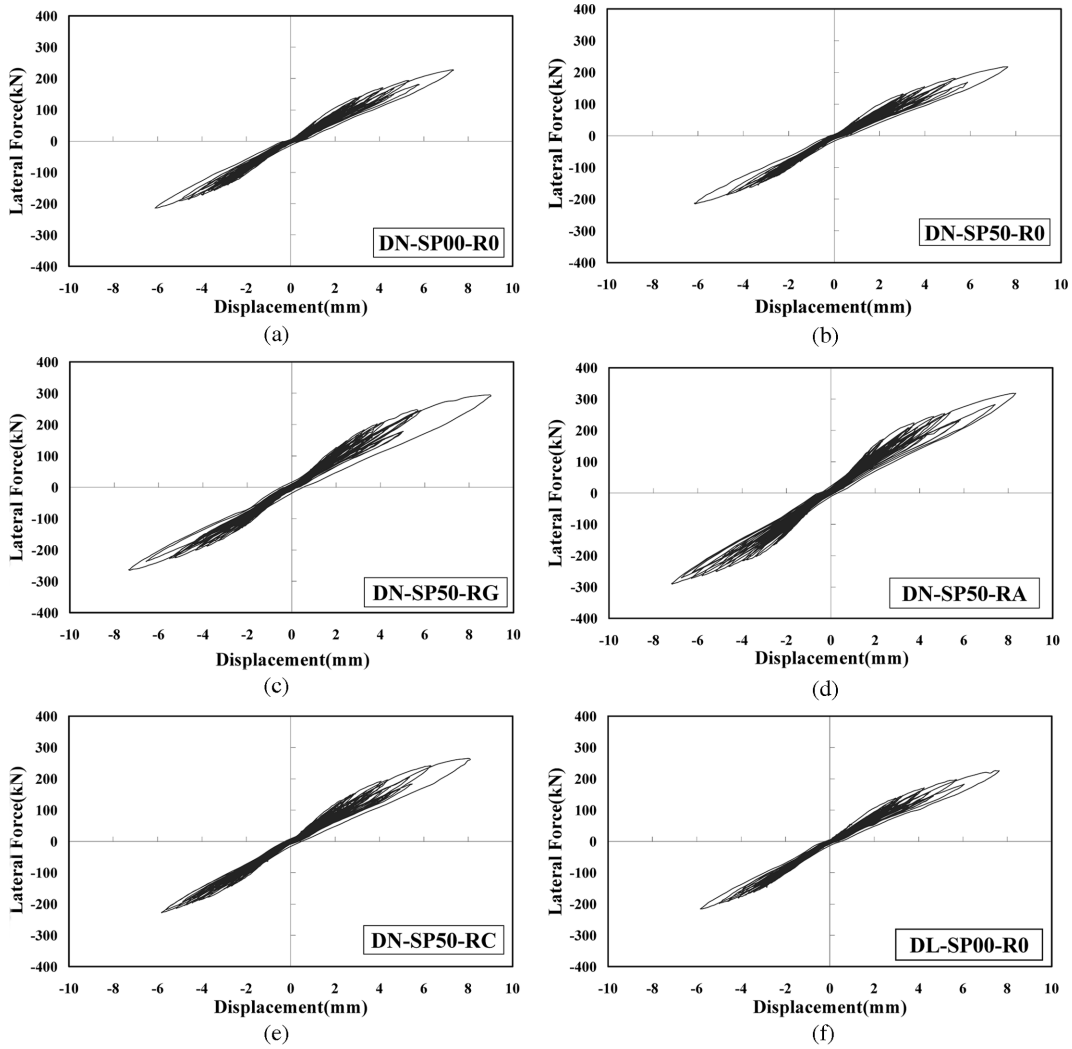

Fig. 5 Lateral force-displacement hysteresis loop under PDT

In the three retrofitted specimens DN-SP50-RA, DN-SP50-RC, and DN-SP50-RG, tearing off of fiber sheets was observed at 5% drift. These retrofitted specimens with aramid, carbon, glass specimens showed fracture of longitudinal steel at 6.0%, 7.0%, and 7.0% drift, respectively.

Specimen US-SP00-R0 had an initial failure pattern similar to specimen DL-SP00-R0. After 6.0% drift, longitudinal bar began to fracture and the specimen failed at 7.0% drift. Most specimens failed in a flexural mode except for the two specimens UN-SP00-R0 and DN-SP00-R0, which showed a flexural-shear failure mode.

Hysteretic behaviors of all test specimens under the quasi-static test are shown in Figs. 6(a)~(f). As shown in Figs. 6(a) and 6(b), undamaged test specimen UN-SP00-R0 had a higher lateral capacity up to 3.0% drift, than that of damaged test specimen DN-SP00-R0. Both specimens UN-SP00-R0 and DN-SP00-R0 exhibited sudden decrease in lateral capacity due to shear failure at 4.0% and 6.0% drift, respectively. The three retrofitted specimens caused higher lateral forces than

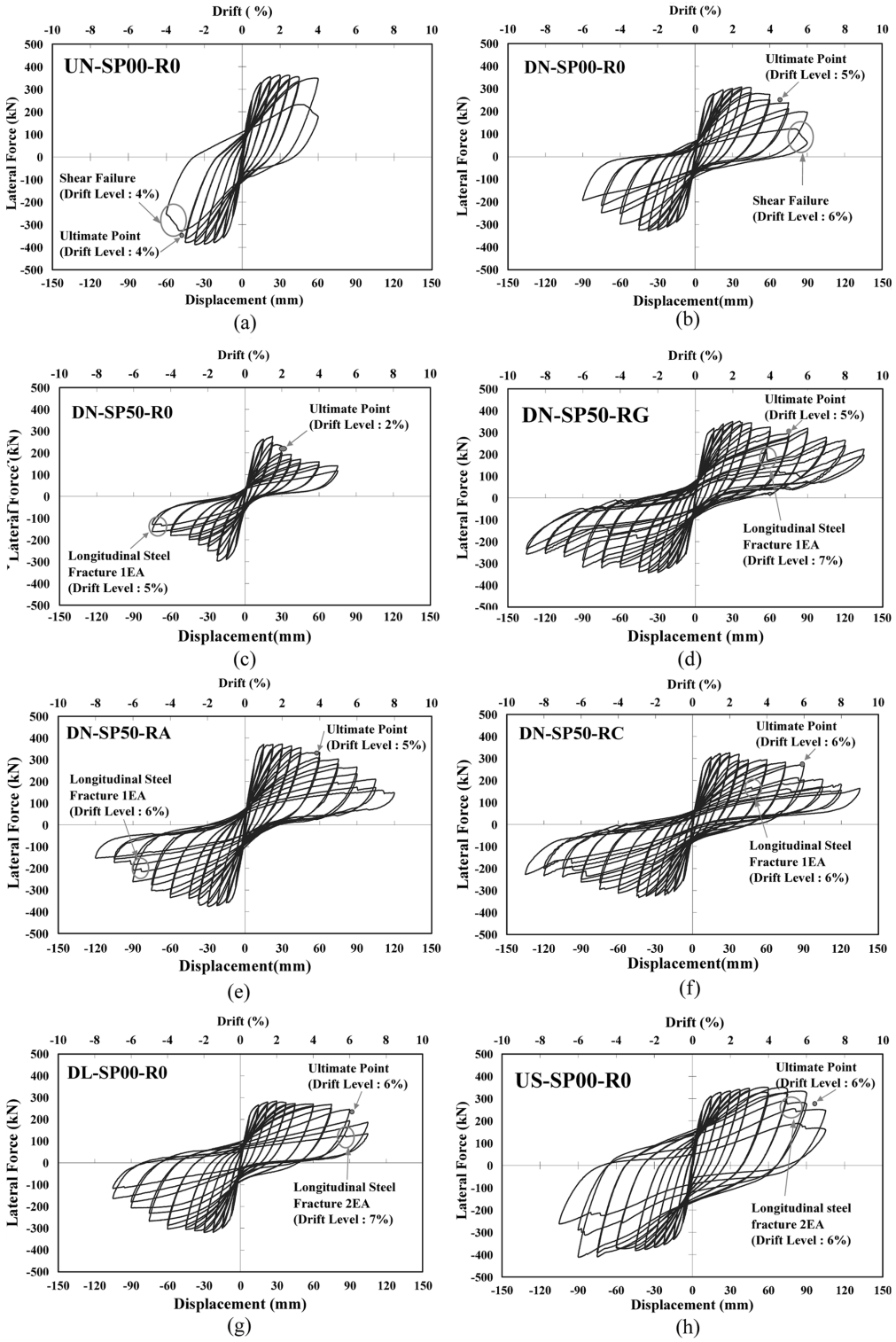

Fig. 6 Lateral force-displacement hysteresis loop under QST

that of the non-retrofitted specimen DN-SP50-R0. As shown in Figs. 6(b) and 6(c), the non-seismic test specimen DN-SP00-R0 without lap splices developed more ductile hysteresis loops than the non-seismic test specimen DN-SP50-R0 with lap splices. As indicated in Figs. 6(c), (d), (e), and (f), it was observed that fiber sheets remarkably increased displacement ductility. Figs. 6(a), (b), (g) and (h) show that as the space of transverse reinforcement steels decreases, a higher displacement ductility is observed. Seismic specimen US-SP00-R0 showed the most stable behavior and energy absorption capacity of all specimens.

3.2 Displacement ductility

Figs. 7(a)~(d) show comparative lateral force-displacement envelope curves for all test specimens with four different parameters; earthquake damage level, transverse confinement, lap splice, and retrofit. As shown in Fig. 7(a), damaged specimen DN-SP00-R0 showed less yield and maximum lateral force than those of the undamaged specimen UN-SP00-R0, but DN-SP00-R0 had a larger ultimate displacement by 15% than UN-SP00-R0. Fig. 7(b) implies that denser transverse confinement steels in the plastic hinge region of RC bridge columns gives bigger ductility.

As shown in Table 4, seismic specimen US-SP00-R0 had a 1.91 times greater ultimate displacement than that of the non-seismic specimen UN-SP00-R0. Moreover, limited ductile

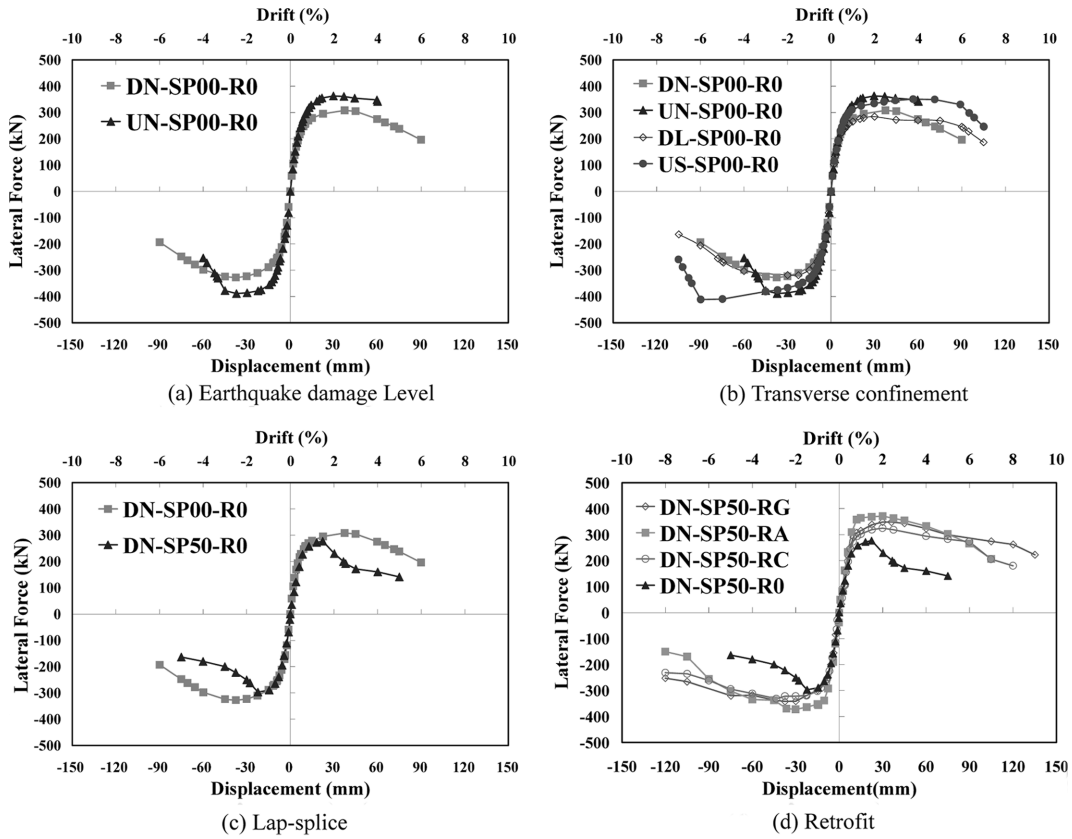

(a) Earthquake damage Level (b) Transverse confinement

(c) Lap-splice (d) Retrofit

Fig. 7 Lateral force-displacement envelope curve under QST

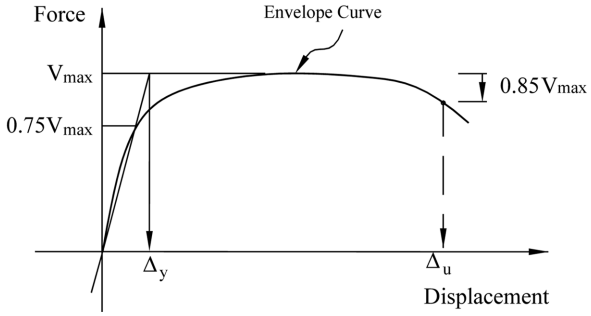

Fig. 8 Definition of yield and ultimate displacement

specimen DL-SP00-R0 had a 39.4% higher ultimate displacement compared to that of the specimen DN-SP00-R0.

A significant reduction of displacement ductility was observed in test specimen DN-SP50-R0 with lap-spliced longitudinal bars, as shown in Fig. 7(c). In addition, lap-spliced specimen DN-SP50-R0 showed a rapid decrease in strength, while specimen DN-SP00-R0 without a lap splice showed a gradual decrease in lateral strength. Fig. 7(d) shows the effect of retrofitting FRP, which considerably increases the strength and displacement ductility of retrofitted columns with lap splices to reach the strength and displacement ductility of the limited ductile specimen DL-SP00-R0.

To minimize major damage and to ensure the survival of structures with moderate resistance with respect to lateral force, structures must be capable of sustaining their initial strength when a major earthquake imposes large deformations.

As shown in Fig. 8, the ultimate displacement Δ_u was defined as the smaller value between the maximum experienced displacement when longitudinal or confinement steel exceeds its fracture state, and the displacement when the strength on the descending branch of force-displacement envelope curve becomes less than $0.85V_{\max}$. The yield displacement Δ_y was defined as the displacement of the intersection point of following two lines: the straight line that passes through the origin and $0.75V_{\max}$ of the envelope curve, and the horizontal line that passes $V_{\max}$ on the envelope curve.

Results of displacement ductility, $\mu_\Delta = \Delta_u/\Delta_y$, are shown in Table 4. Three retrofitted specimens DN-SP50-RG, DN-SP50-RA, and DN-SP50-RC increased displacement ductility by 2.7~3.4 times with respect to the corresponding reference test specimen DN-SP50-R0. Displacement ductility ratio of lap-spliced test specimen DN-SP50-R0 was significantly reduced to approximately 0.4 times that of the reference specimen DN-SP00-R0. The damaged specimen DN-SP00-R0 showed bigger displacement ductility compared to the undamaged specimen UN-SP00-R0. It was thought from these results that shear failure of both specimens DN-SP00-R0 and UN-SP00-R0 gave less reliable displacement ductility.

3.3 Energy absorption capacity

Fig. 9 shows comparative curves of the cumulative energy absorption capacity of all test specimens with four test parameters. The amount of absorption energy in each load cycle was calculated from the hysteresis loop.

Table 4 Displacement ductility under QST

Specimen	Yield		Ultimate		Displacement ductility ($\mu_\Delta = \Delta_u/\Delta_y$)
	Force (kN)	Displacement (mm)	Force (kN)	Displacement (mm)	
UN-SP00-R0	307.1	11.60	330.6	49.71	4.28
DN-SP00-R0	265.8	10.82	265.7	66.00	6.10
DN-SP50-R0	241.8	9.82	300.0	24.08	2.45
DN-SP50-RA	343.5	9.50	322.2	70.00	7.37
DN-SP50-RG	309.1	11.19	305.6	74.93	6.70
DN-SP50-RC	289.4	10.65	282.1	88.00	8.26
DL-SP00-R0	248.1	10.13	245.1	92.00	9.08
US-SP00-R0	292.2	11.38	298.2	95.10	8.36

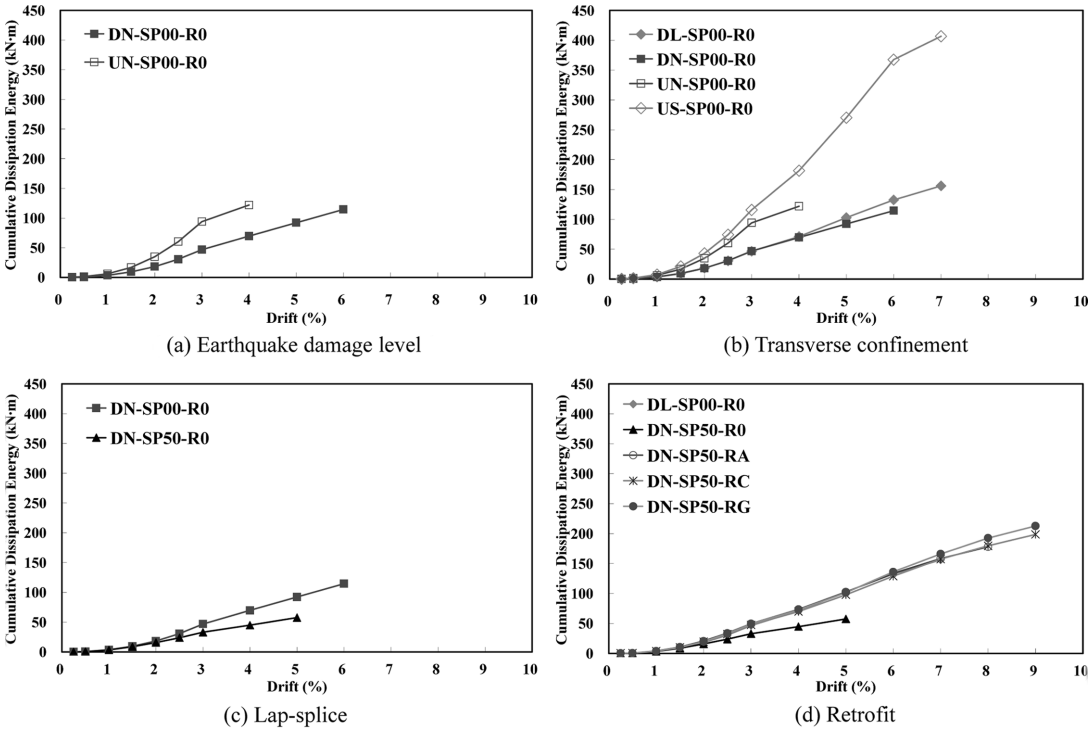

Fig. 9 Cumulative dissipation energy

As shown in Fig. 9(a), compared to damaged specimen DN-SP50-R0, the undamaged specimen UN-SP00-R0 showed a 75% higher energy absorption capacity at 4% drift level before shear failure. Fig. 9(b) shows that increased transverse confinement in the plastic hinge region gave bigger energy absorption capacity. It was also found from Fig. 9(c) that the energy absorption capacity of test specimen DN-SP50-R0 with a lap splice of 50% longitudinal reinforcement bars was decreased by about 50% than that of the non-spliced specimen DN-SP00-R0. Fig. 9(d) shows that energy

absorption capacities of retrofitted specimens DN-SP50-RA, DN-SP50-RC, and DN-SP50-RG with FRP sheets were increased by more than 210%, compared to that of the non-retrofitted test specimen DN-SP50-R0, and were similar to that of the limited ductile specimen DL-SP00-R0.

4. Damage assessment

Damage index has a potential to play a vital role in retrofit decision-making, disaster planning, and evaluation of residual seismic performance in earthquake regions. In order to estimate resistance of specific structures to seismic events, damage must be measurable and predictable. Damage index provides a means to quantify damage, economic loss, and other consequences such as potential risk after an earthquake. In this research, damage index was computed by Eq. (4) as shown below. This equation that combines a simple displacement ductility term with hysteretic energy absorption was developed by Park and Ang (1985).

$$D = \frac{\delta_M}{\delta_u} + \frac{\beta}{Q_y \delta_u} \int dE \tag{4}$$

where, δ_M = Maximum deformation under earthquake; δ_u = ultimate deformation under monotonic loading; Q_y = calculated yield strength; dE = incremental absorbed hysteretic energy; and β = coefficient for cyclic loading effect. The β value of Eq. (4) was calculated by assuming the damage index $D = 1.0$ at ultimate displacement defined in section 3.2. Resulting β values for all specimens are shown in Table 5.

Table 5 Damage indices

Test load \ Specimen		UN-SP00 -R0	DN-SP00 -R0	DN-SP50 -R0	DN-SP50 -RA	DN-SP50 -RG	DN-SP50 -RC	DL-SP00 -R0	US-SP00 -R0
PDT	0.0803 g	-	0.045	0.108	0.031	0.026	0.032	0.034	-
	0.11 g	-	0.059	0.144	0.050	0.043	0.049	0.044	-
	0.154 g	-	0.076	0.206	0.073	0.061	0.071	0.059	-
	0.22 g	-	0.104	0.304	0.113	0.094	0.092	0.080	-
QST	0.25%	0.067	0.104	0.304	0.113	0.094	0.092	0.080	0.036
	0.5%	0.133	0.109	0.316	0.113	0.094	0.092	0.080	0.072
	1.0%	0.269	0.216	0.628	0.204	0.159	0.175	0.157	0.145
	1.5%	0.411	0.327	1.000	0.308	0.241	0.269	0.237	0.220
	2.0%	0.561	0.441	-	0.417	0.326	0.371	0.318	0.297
	2.5%	0.720	0.560	-	0.531	0.413	0.480	0.400	0.376
	3.0%	0.888	0.684	-	0.649	0.503	0.596	0.484	0.458
	4.0%	1.000	0.919	-	0.873	0.676	0.808	0.648	0.618
	5.0%	-	1.000	-	1.000	0.854	1.000	0.815	0.784
	6.0%	-	-	-	-	1.000	-	0.980	0.952
	7.0%	-	-	-	-	-	-	1.000	1.000
	β	0.016	0.012	0.130	0.019	0.012	0.036	0.005	0.007

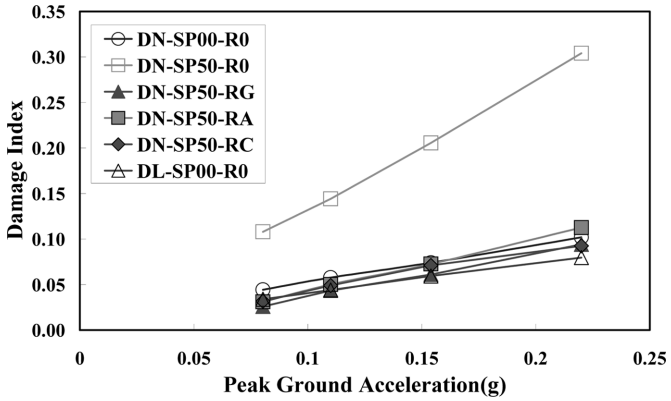

Fig. 10 Damage indices under PDT

4.1 Pseudo dynamic test

To simulate probable earthquake damage, six specimens went through the PDT by loading four series of artificial earthquakes. After the PDT, these specimens were damaged as shown in Table 5. The damage state could be represented as the Damage Index (DI), which was proposed by Park and Ang (1985). Though un-retrofitted lap-spliced specimen DN-SP50-R0 elastically behaved as shown in Fig. 5(b), it showed a relatively high damage index of 0.3041, which was about three times of DN-SP00-R0 without a lap-splice. Retrofitted specimens DN-SP50-RG, DN-SP50-RA, and DN-SP50-RC with a lap-splice showed a similar damage index to DN-SP00-R0 without a lap-splice. Most specimens except for the un-retrofitted and lap-spliced specimen DN-SP50-R0 showed a damage index about 0.1, which is generally considered to be a repairable damage state. Fig. 10 shows damage indices for all test specimens. Three retrofitted specimens DN-SP50-RG, DN-SP50-RA, and DN-SP50-RC showed relatively high maximum displacements, but had a lower damage index. In addition, it is evident that lap-splices are one of the crucial factors for the seismic performance as well as for the damage of RC columns.

4.2 Quasi static test

Damage index results for QST are shown in Fig. 11. Computed damages for all specimens were in relatively good agreement with test observations. After the pseudo-dynamic test, specimen DN-SP50-R0 had an approximately 0.3 damage index which was close to the damage index of other specimens at 2.0% drift of the QST. Damage indices of retrofitted specimens were significantly reduced compared to the un-retrofitted specimen. When retrofitted specimens were reinforced with FRP wrap, damage reduced to one-third at 0.25% drift. As shown in Figs. 11(a) and (b), both specimens showed similar damage states. Up to 0.5% drift, the damaged specimen showed minor damage as compared to the undamaged specimen.

All test specimens showed gradual increase in damage except for specimen DN-SP00-R0. Figs. 11(a), (b), (g), and (h) showed that test specimens with increased confinement reinforcement steels possibly had lower damage indices. Very similar damages were observed for specimens DN-SP00-RG, DN-SP00-RA, and DN-SP00-RC. More confined specimens DL-SP00-R0 and US-SP00-R0 showed significant improvement of the damage index.

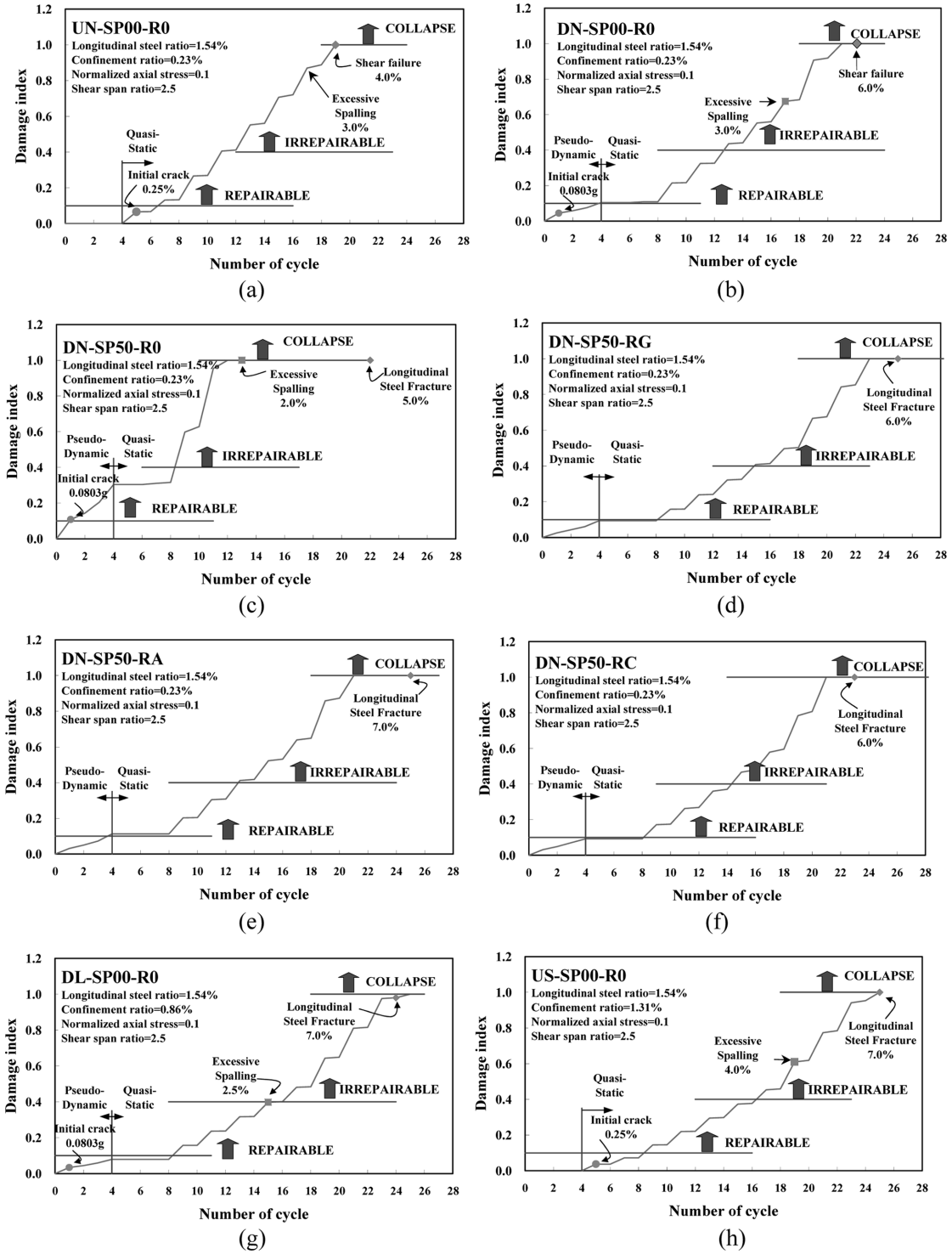

Fig. 11 Damage index under QST

5. Conclusions

Test results showed that specimens damaged under a series of probable earthquake ground motions had good residual seismic performance, and that retrofitting RC bridge columns wrapped with fiber composites in the potential plastic hinge region was an effective retrofitting measure to enhance flexural ductility. Lap-spliced RC pier specimens were especially vulnerable and need to be retrofitted to secure good seismic performance under probable earthquakes. The following conclusions can be made.

a) Even under the 0.22 g earthquake motions in the pseudo dynamic test, all test specimens except for the un-retrofitted and lap-spliced specimen behaved almost linearly with minor damage.
b) Non-seismically designed RC bridge piers with lap spliced longitudinal reinforcement bars in the plastic hinge region, appeared to fail at much lower displacement ductility than those without lap splices.
c) Retrofitting material considerably increased the lateral strength and displacement ductility of retrofitted specimens, which reached the capacity of the limited ductile specimen.

Since the Korean peninsula is considered to be a low or moderate seismic region, RC bridge piers now in service, that were constructed with 50% longitudinal bars lap-spliced in accordance with the pre-1992 design code, could satisfy seismic requirements of the KHBDS if these RC columns were appropriately retrofitted with FRP wraps.

Acknowledgements

The authors gratefully acknowledge the support from the Korea Earthquake Engineering Research Center (Contract No. R11-1997-045-12005-0).

References

AASHTO (2004), "AASHTO LRFD bridge design specification", American Association of State Highway and Transportation Officials, USA.

Aboutaha, R.S., Engelhardt, M.D., Jirsa, J.O. and Kreger, M.E. (1999), "Experimental investigation of seismic repair of lap splice failures in damaged concrete columns", *ACI Struct. J.,* **96**(2), 297-307.

Chai, Y., Priestley, M.J.N. and Seible, F. (1991), "Seismic retrofit of circular bridge columns for enhanced flexural performance", *ACI Struct. J.,* **88**(5), 572-584.

Chang, S.P., Kim, J.K., Kim, I.H. and Lim, H.W. (2000), "The influence of lap splice of longitudinal bars in the plastic hinge zone on the nonlinear behavior characteristics of RC piers and new seismic detailing concept in moderate seismicity region," *Proc. the Earthq. Eng. Soc. Korea Conf.*, **4**(1), 335-340.

Chung, Y.S., Lee, K.K., Han, G.H. and Lee, D.H. (1999), "Quasi-static test for seismic performance of circular R.C. bridge piers before and after retrofitting", *J. of the Korea Concrete Institute*, **11**(5), 107-118.

Chung, Y.S., Park, C.K. and Lee, E.H. (2004), "Seismic performance and damage assessment of reinforced concrete bridge piers with lap-spliced longitudinal steels", *Struct. Eng. Mech.*, **17**(1), 51-68.

Einea, A., Yehia, S. and Tadros, M.K. (1999), "Lap splices in confined concrete", *ACI Struct. J.*, **96**(6), 947-955.

El-Bahy, Ashraf, Kunnath, Sashi, Stone, William, and Taylor, Andrew (1999), "Cumulative seismic damage of circular bridge columns : Variable amplitude tests", *ACI Struct. J.,* **96**(5), 711-720.

Jaradat, O.A., McLean, D.I. and Marsh, M.L. (1998), "Performance of existing bridge columns under cyclic loading - Part 1: Experimental results and observed behavior", *ACI Struct. J.,* **95**(6), 695-704.

KHBDS (2000), "Korea highway bridge design specification", Korea Road & Transportation Association, Ministry of Construction and Transportation.
Lehman, D.E., Gookin, S.E., Nacamuli, A.M. and Moehle, J.P. (2001), "Repair of earthquake-damaged bridge columns", *ACI Struct. J.*, **98**(2), 233-242.
Melek, Murat and Wallace, John W. (2004), "Cyclic behavior of columns with short lap splices", *ACI Struct. J.,* **101**(6), 802-811.
Park, Y.J. and Ang, Alfredo H-S. (1985), "Mechanistic seismic damage model for reinforced concrete", *J. of Struct. Eng.,* **111**(4), 722-739.
Priestley, M.J.N., Seible, F. and Calvi, G.M. (1996), *Seismic Design and Retrofit of Bridges,* John Wiely & Sons Inc., New York.
Saadatmanesh, H., Ehsani, M.R. and Jin, L. (1996), "Seismic strengthening of circular bridge pier models with fiber composites", *ACI Struct. J.,* **93**(6), 639-647.
Seible, F., Priestley, M.J.N., Hegemier, G.A. and Innamorato, D. (1997), "Seismic retrofit of RC columns with continuous carbon fiber jackets", *J. of Composites for Construction*, **1**(2), 52-62.